The International Journal of Advanced Manufacturing Technology (2019) 103:1459–1466
https://doi.org/10.1007/s00170-019-03640-2

ORIGINAL ARTICLE

Investigation of redistribution mechanism of residual stress during multi-process milling of thin-walled parts

Miaoxian Guo[1] · Xiaohui Jiang[1] · Yi Ye[1] · Zishan Ding[1] · Zhenya Zhang[1]

Received: 12 October 2018 / Accepted: 26 March 2019 / Published online: 5 April 2019

Abstract

Applications of thin-walled parts are substantially affected by residual stress generated during the cutting process. However, in multi-process milling, the redistribution mechanisms of residual stress after roughing, semi-finishing, finishing, and heat treatment are highly complex and remain underexplored. As a result, the control of deformation of multi-process thin-walled parts remains challenging. In this study, to reduce the influence of residual stress on the deformation of complex thin-walled parts, simulation models of the machining process and heat treatment are carried out based on multi-process analysis. By comparing different process parameters, the redistribution mechanism of residual stress during multi-process milling is analyzed. The findings reveal that with a stress-relief treatment between every process, especially before finishing machining, compressive stress on the surface of thin-walled parts is greatly reduced; residual stress on the sub-surface enters a stable state quickly; and the internal metal structure and structural performance are more reliable. Experiments are conducted to verify these results by comparing residual stress. Stress-relief treatment after every cutting process is ultimately recommended for controlling residual stress and deformation of thin-walled parts in multi-process machining.

Keywords Residual stress · Redistribution mechanism · Thin-walled parts · Multi-process milling · Deflection

1 Introduction

With the advantage of being lightweight, thin-walled parts have been widely applied in industries including automotive, aerospace, and precision machinery. However, due to the machining complexity of thin-walled parts, applications encounter problems of residual stress, cutting force, heat, clamping force, and vibrations. More requirements are involved in the distribution of residual impact stress on surfaces and sub-surfaces that affect workpiece performance on the premise of meeting machining precision. Thin-walled parts with complex structures that require multi-process milling especially result in the redistribution of residual stress, which is difficult to characterize and control in research.

To understand the profile of residual stress in the multi-process milling of thin-walled parts, several researchers have carried out investigations on machined residual stress by simulation and experiment [1, 2]. To analyze and study the redistribution mechanism of residual stress during multi-process milling of thin-walled parts, distribution mechanisms of residuals have been analyzed in a single process by considering different processing parameters, tool parameters, and other factors. Processing parameters during machining are considered main factors that influence residual stress generation. Arrazola et al. [3] pointed out the need to investigate the effects of cutting conditions, tool parameters, and cooling conditions on residual stresses in the machined surface layer. Coto et al. [4] found that a higher feed rate would increase the magnitude of tensile residual stress, and less tensile residual stress was generated by increasing the cutting speed. Navas et al. [5] noted that by reducing the feed rate and increasing the cutting speed, less tensile residual stress was achieved in AISI4340 steel. Li et al. [6] completed the milling process using a residual stress analysis on turning, which could be easily performed as a two-dimensional (2D) orthogonal cutting process, despite the original process being regarded as a typical three-dimensional (3D) oblique cutting process. Then, a 2D fully thermo-mechanical coupled FE model was proposed to study residual stress induced by high-speed end-

✉ Miaoxian Guo

[1] School of Mechanical Engineering, University of Shanghai for Science and Technology, Shanghai 200093, China

milling of hardened steel SKD11. Based on model analysis, Masoudi et al. [7] studied the mechanism and effective parameters of deformation in machining thin-walled workpieces by applying different processing parameters in an engineering test. Huang et al. [8] developed a method of parameter inversion in geophysics to compute residual stress profiles, presenting a new way to achieve desired residual stress. Jiang et al. [9] found that the residual impact stress on multiple machined surfaces can be decreased by increasing the cutting speed. Yang et al. [10] investigated the coupled distribution of initial and machining-induced residual stress and found that the effect of coupled stress distribution is significant with the decrease of thickness of the thin-walled parts.

Tool parameters have also been well investigated using theoretical and experimental methods. Tool edge geometry has been found to exert significant effects on the cutting process. Kazban [11] pointed out that residual stress tended to decline as the tool edge radius increased when using a fluid mechanics approach and measurement. Mohamend et al. [12] also found a larger tool edge radius to induce higher tensile residual stress in the near-surface layer while it induced higher compressive residual stress far from the surface. Lin et al. studied the effect of tool flank wear length on residual stress profiles in machining. Tang et al. [13] found that tool flank wear exerts a significant effect on superficial residual stress, whereas small flank wear produces a lower tensile or compressive stress on the surface, and stress transitions to a tensile state with an increase in flank wear. An experimental study of the influence of tool wear in residual stresses is difficult due to the need to control wear evolution during cutting. Therefore, Muñoz-Sánchez et al. [14] introduced a numerical model to analyze the tool wear effect in machining-induced residual stress. Based on this approach, Huang et al. [15] took processing parameters and tool parameters into account to reveal the mechanisms behind the effects of machining parameters and tool parameters on residual stress. What's more, Jiang et al. [16] studied the residual stress redistributes in the surface and sub-surface of parts during the machining, and found that the tool overlap affections are critical to deflection of the thin-walled parts and residual stress.

Part machining can be divided into roughing, finishing, heat treatment, and other processes; the above studies focused mostly on single-process residual stress distribution. Furthermore, many studies have investigated the redistribution of residual stress with sequential cuts, which can be traced back to research in the 1950s. Treuting and Read [17] established a relationship

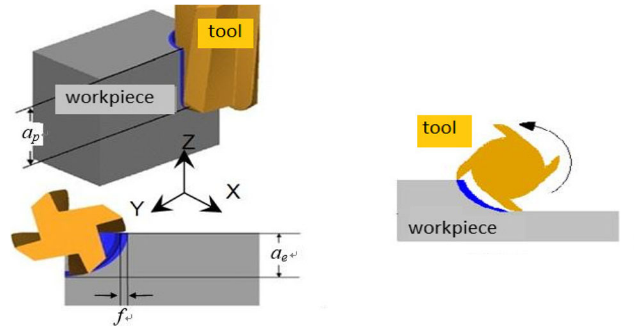

Fig. 1 Simulation model of milling process (Third Wave Systems, 2010).

between stress and curvature by removing sheet material layer by layer, paving the way for analysis of the redistribution of residual stress and deformation. In recent years, to simulate the multi-cutting effects on residual stress in a machined layer, Liu et al. [18] developed a thermo-elastic-plastic coupling FEM model; simulation results indicated that machined surface residual stress could be changed from tensile stress to compressive stress by optimizing the second cutting process. Lee and Nikbin [19] selected workpieces with different geometric shapes to study the influence of the stress-sensitive factor for different structures during heat relief. Based on measurements and finite element analysis prediction, Robinson et al. [20] analyzed the redistribution law of residual stress in cutting Al 7449 by removing material layer by layer. Li et al. [21] investigated the redistribution mechanisms of residual stress and deformation by using different depths of cut. Results showed that, in roughing, by selecting a subsequent depth exceeding the prior depth of the maximum compressive residual stress, material can be removed in favor of subsequent machining, in finishing, different depths of cut are utilized in different cutting stages, resulting in a smaller magnitude of a maximum machined residual stress and depth of maximum compressive residual stress.

These residual stress works are based on a single-process analysis. As in redistribution studies, limited research has involved multi-process milling of thin-walled parts. Therefore, it is difficult to apply a redistribution mechanism of residual stress in thin-walled part analysis. To further analyze the redistribution of residual stress of thin-walled parts in multi-process milling, this study carried out a semi-finishing and finishing simulation in the Third Wave AdvantEdge [22] model and a heat treatment simulation for destressing in the heat treatment module of ABAQUS [23], to reveal the

Table 1 Material composition of Al 7050 (mass, %)

Zn	Mg	Cu	Si	Fe	C	Mn	Cr	Zr	Ti	Al
6.2	2.3	2.3	0.12	0.15	0.12	0.10	0.04	0.115	0.06	bal.

Table 2 Process parameters of milling process

Process	V(rpm)	a_p(mm)	a_e(mm)	f(mm/tooth)
Semi-finishing	1400	0.3	1	0.2
finishing	1800	0.1	1	0.1

Table 3 Material properties of Al 7050 in different temperature fields

Temperature (°C)	Density (kg/m^3)	Thermal diffusivity (m^2/s)	Young's modulus (N/m^2)	Poisson ratio	Coefficient of thermal expansion (1/°C)	Specific heat capacity (J/(kg°C)	Yield stress (MPa)
20	2796	145	7.3×10^{10}	0.33	0	852	266
180	2783	156	7.1×10^{10}	0.338	7.8×10^{-6}	862	246

superposition distribution regularity of residual stress in multi-process machining. At last, a machining experiment is conducted to verify the simulation, providing a theoretical basis and engineering experience for controlling residual stresses and deformation of thin-walled parts in multi-process milling.

2 Simulation procedure

2.1 Process analysis

The structure and machining process of thin-walled parts used in industries are complex, especially for aluminum alloy thin-walled parts. To study the redistribution mechanism of residual stress during multi-process milling, a flat frame part is applied in our simulation and experiment, involving a process of initial heat treatment → roughing → semi-finishing → stress-relief heat treatment → finishing → stress-relief heat treatment. Then, residual stress in multi-machining with or without stress-relief heat treatment is compared, and a verification test is carried out with aluminum alloy thin-walled parts based on a multi-processing procedure.

2.2 Modeling of milling process

Several models of residual stress in machining have been developed in research. Ulutan et al. [24] and Lazoglu et al. [25] developed an enhanced analytical model for residual stress prediction in machining. Liang et al. [26] modeled residual stress in orthogonal machining. In this paper, to analyze the redistribution mechanism of residual stress, an FE simulation of cutting is used to predict residual stress. Based on the Third Wave Advanced Edge model, the cutting process of Al7050 (Table 1) is simulated with initial residual stress. The simulation model is shown in Fig. 1, and process parameters are listed in Table 2. Furthermore, as displayed in Eq. (1), the model power law is selected with the flow stress curve defined in the material library of AdvantEdge™.

$$\sigma\left(\varepsilon^{p}, \dot{\varepsilon}, \mathrm{T}\right) = \mathrm{g}(\varepsilon^{p})\cdot\Gamma\left(\dot{\varepsilon}\right)\cdot\Theta(\mathrm{T}) \quad (1)$$

where $\mathrm{g}(\varepsilon^{p})$ is strain hardening, $\Gamma(\dot{\varepsilon})$ is strain rate sensitivity, and $\Theta(\mathrm{T})$ is thermal softening.

2.3 Modeling of heat treatment

Heat treatment is a process used to alter the physical (and occasionally chemical) properties of a material. The heat treatment problem in this process can be defined as an unsteady heat conduction problem, and the Fourier thermal conductivity differential equation is

$$\lambda\left(\frac{\partial^2 T}{\partial x^2} + \frac{\partial^2 T}{\partial y} + \frac{\partial^2 T}{\partial z^2}\right) + \sigma\dot{\varepsilon}_{ij}^{P} - \sum_{l=0}^{N}\rho_l L_l \frac{\partial \xi_l}{\partial t} = \rho c \frac{\partial T}{\partial t} \quad (2)$$

where T is temperature, t is time, λ is the coefficient of thermal conductivity, σ is stress, $\dot{\varepsilon}_{ij}^{P}$ is the plastic strain rate, ρ is density, L is the latent heat generated by phase transformation, and c is the heat capacity at a constant pressure.

To analyze the overlap of heat treatment on machined residual stress, a workpiece model with residual stress load is imported into Abaqus CAE software. The material properties

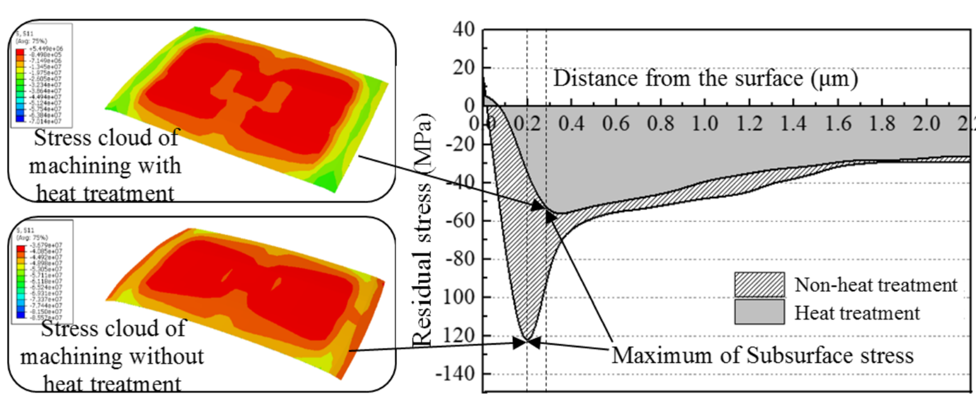

Fig. 2 Residual stress—σ_{xx} comparison in semi-finishing process

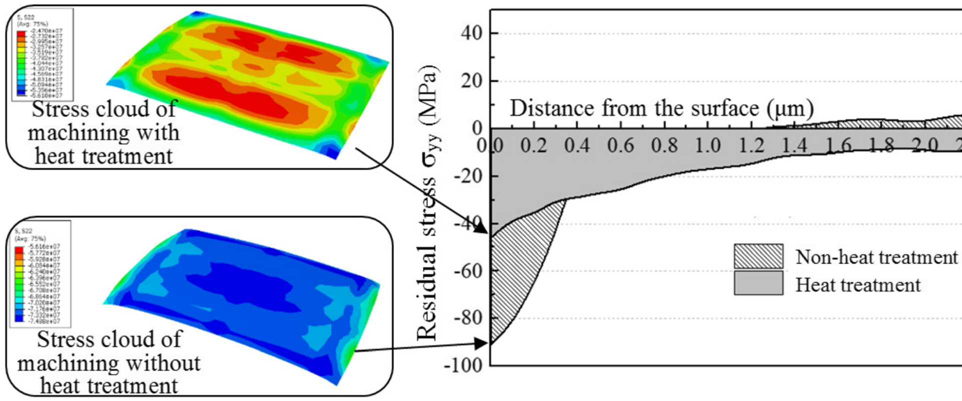

Fig. 3 Residual stress—σ_{yy} comparison in semi-finishing process

of a thin-walled aluminum alloy in different temperature fields are described in Table 3.

The heat treatment process after semi-finishing and finishing cutting processes was set up in the software as follows: (1) semi-finishing heat treatment, in which the workpiece is heated from 20 to 180 °C at 0.25h, and the temperature is then maintained at 180 °C for 2.5 h before being cooled naturally to 20 °C in 1/6 h; (2) finishing heat treatment, in which the workpiece is heated from 20 to 140 °C at 0.25 h, and the temperature is then maintained at 140 °C for 2.5 h before being cooled naturally to 20 °C in 1/6 h. Residual stress and deformation are then calculated.

3 Results and discussion

In multi-process milling, the redistribution mechanism of residual stress after semi-finishing, finishing, and heat treatment are important in the machining precision of thin-walled parts. According to different machining procedures in multi-process milling of thin-walled parts, the redistribution of the residual stress is discussed along the distance from the surface; deformation is compared in the *X*-/*Y*-directions (*X* feeding direction, *Y* vertical feeding direction).

3.1 Superposition of residual stress in semi-finishing and heat treatment

Figure 2 shows the distribution of residual stress in the feeding direction (σ_{xx}) at a depth of 2.2 μm. The grid area is the distribution of σ_{xx} from the surface to the sub-surface in semi-finishing, and the gray area is the distribution of σ_{xx} in semi-finishing cutting with heat treatment. Residual stress on the surface of the workpiece is tensile stress, and the subsurface residual stress is compressive stress. Furthermore, a comparison of residual stress indicates that σ_{xx} in semi-finishing cutting with heat treatment appears to drop suddenly, with the maximum reducing by 54% and an average decline of approximately 20%. With an increase in distance from the

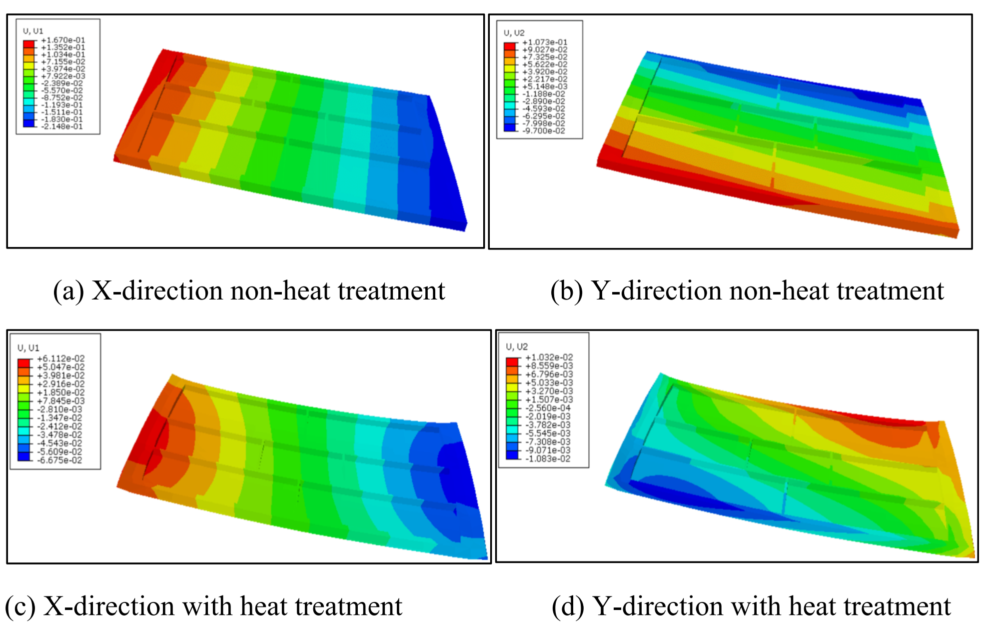

Fig. 4 Effect of residual stress on deformation in semi-finishing machining. **a** *X*-direction non-heat treatment. **b** *Y*-direction non-heat treatment. **c** *X*-direction with heat treatment. **d** *Y*-direction with heat treatment

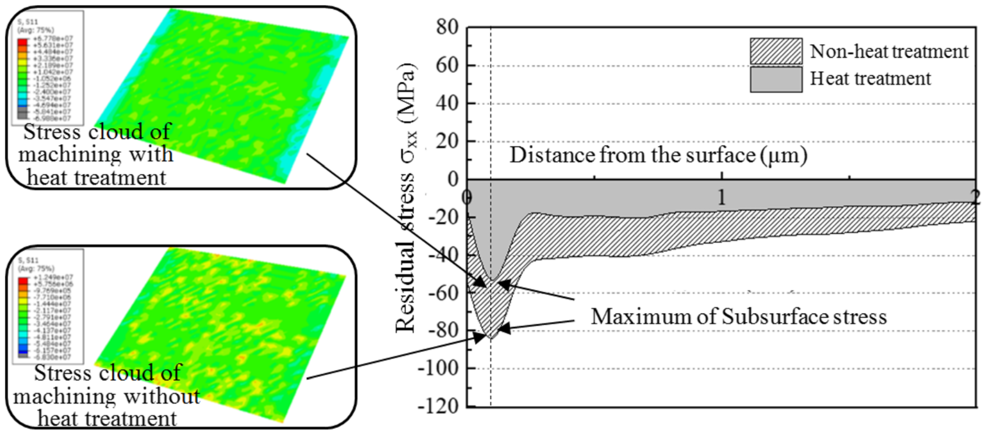

Fig. 5 Residual stress—σ_{xx} comparison in finishing process

surface, the two residual stresses tend to become gradually equal and stable.

Figure 3 shows the distribution of residual stress in the vertical feeding direction (σ_{yy}) at a depth of 2.2 μm. σ_{yy} in the semi-finishing process is compressive stress on the surface, when penetrating deeper into the sub-surface, the residual stress gradually declines and becomes tensile stress. After heat treatment, σ_{yy} is maintained as the compressive stress reduces gradually and tended to stabilize around 10 MPa. σ_{yy} also demonstrates a reduction in compressive stress on the surface of thin-walled parts of approximately 45 MPa (50%) after heat treatment in the semi-finishing process.

3.2 Deformation of thin-walled parts in semi-finishing and heat treatment

In this process, the residual stress exerts a significant influence on the deformation of the part, as shown in Figs. 4 and 5 the effect of residual stress on deformation in semi-finishing machining is studied. Deformations of thin-walled parts in the *X* and *Y* directions are analyzed. Comparing the deformation amplitude between semi-finished parts and semi-finished parts with heat treatment, the *X*-direction deformation of the thin-walled workpiece declines by about 63.4% whereas the *Y*-direction deformation reduces by about 89% after stress-relief treatment. Therefore, the stress-relief heat treatment process appears important in multi-process milling.

3.3 Superposition of residual stress in finishing and heat treatment

The preceding analysis indicates that residual stress can be controlled at a lower level. This section discusses the finishing machining process. In modeling analysis, σ_{xx} and σ_{yy} are extracted from the stable cutting stage. Figs. 6 and 7 indicate that the grid area is the distribution of σ_{xx} and σ_{yy} from the surface to the sub-surface in finishing cutting. Compared with the results of semi-finishing and heat treatment, residual stress on the workpiece surface σ_{xx} increases by about 40%, and the sub-surface residual stress increases by about 5–10%. On the contrary, surface residual stress decreases by around 35%, and the sub-surface residual stress declines to about 5 Mpa.

To investigate the redistribution mechanism of residual stress after the finishing machining process and finally optimize residual stress and deformation, heat treatment is conducted using the finite element method. The residual stresses σ_{xx} and σ_{yy} after finishing cutting are then compared with the final heat treatment σ_{xx} and σ_{yy}. The results show that surface

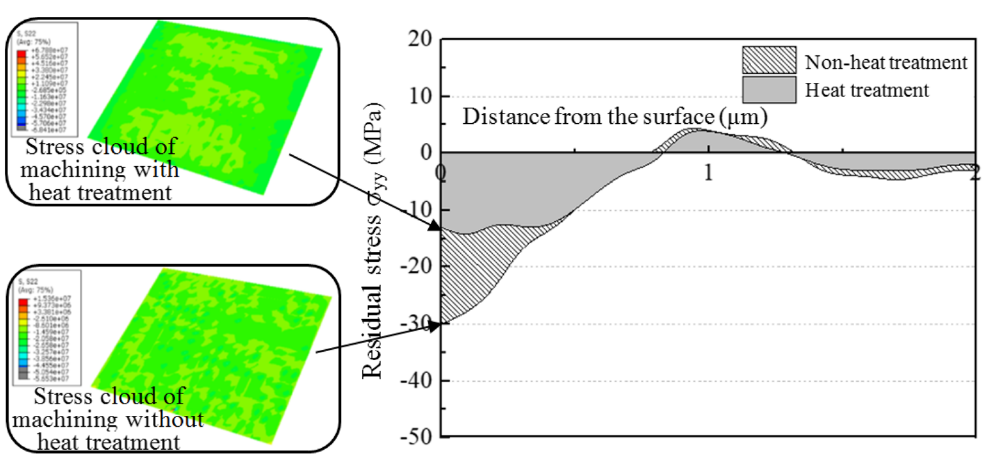

Fig. 6 Residual stress—σ_{yy} comparison in finishing process

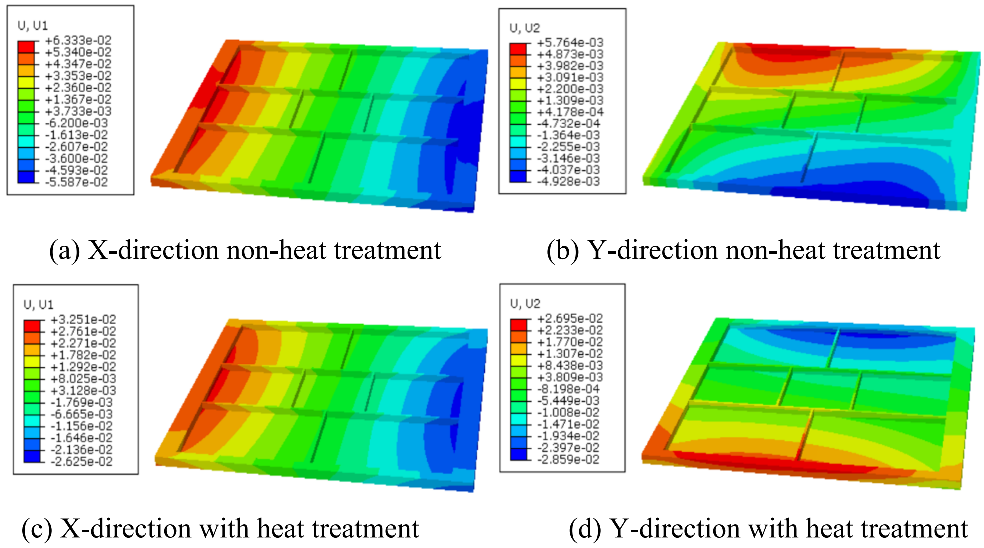

Fig. 7 Effect of residual stress on deformation in finishing machining. **a** *X*-direction non-heat treatment. **b** *Y*-direction non-heat treatment. **c** *X*-direction with heat treatment. **d** *Y*-direction with heat treatment

compressive stress σ_{xx} after heat treatment is reduced by approximately 36.5%, and the maximum sub-surface compressive stress σ_{xx} is reduced by about 30%. σ_{yy} declined by 56.7% after heat treatment, and the maximum sub-surface residual stress of thin-walled parts is 5 Mpa. Moreover, the distribution of sub-surface compressive stress in the *X*-direction is highly stable, ensuring *X*-direction strength of thin-walled parts.

3.4 Deformation of thin-walled parts in finishing and heat treatment

As shown in Table 2, the machining parameters in the finishing process are smaller than those in the semi-finishing process. Therefore, as presented in Fig. 8, the *X*- and *Y*-deformations of thin-walled parts after finishing machining are much smaller than those after semi-finishing cutting. According to the analysis of *X*-direction deformation of thin-walled parts before and after heat treatment, the maximum deformation is reduced by approximately 40% whereas the *Y*-direction deformation declined by around 50%. Finally, after multi-process milling—including semi-finishing, stress-relief heat treatment, finishing, and stress-relief heat treatment—residual stress and deformation are optimized.

4 Experimental validation

To verify the modeling results of the simulation procedure, the experiments are carried out in this section, with relevant results such as residual stress and deformation measured after multi-process milling.

4.1 Experimental setup

As shown in Fig. 8, milling experiments are conducted on Bridgeport machine (Model XR1000), and heat treatment is conducted in a box resistance furnace (SG-1000).

(a) Milling machine (b) Heat-treatment instrument

Fig. 8 Experimental setup. **a** Milling machine. **b** Heat treatment instrument

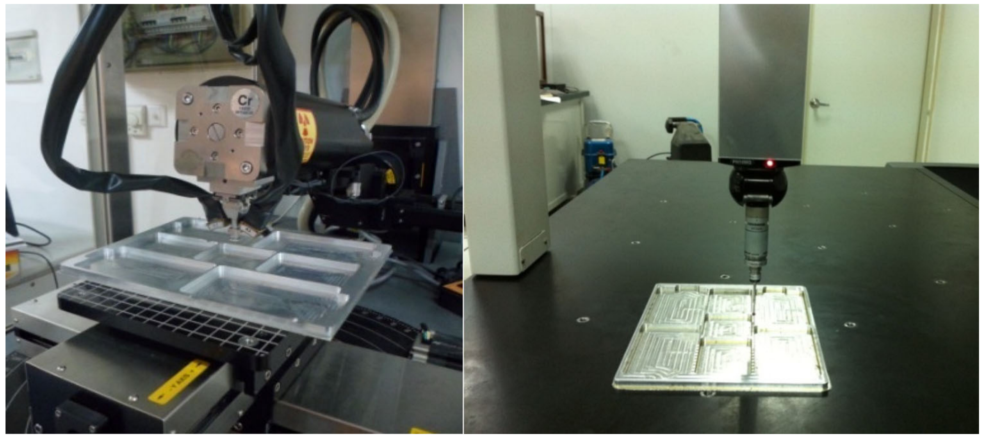

(a)) X-ray stress analyzer (b) Coordinate measurement machine

Fig. 9 Measurement setup. **a** X-ray stress analyzer. **b** Coordinate measurement machine

The process parameters adopted in this experiment are presented in Tables 1 and 3. Residual stress on the workpiece surface is measured and analyzed during milling, and the X-ray method is applied to avoid damage to the workpiece. Thus, in this study, a high-powered Canada PROTO (Fig. 9a) residual stress analyzer (LXRD) is employed to measure machined residual stress. After finishing, based on the reference plane, the coordinate of the machined thin-walled part is measured on the coordinate measurement machine Global Performance 7107 (Fig. 9b).

4.2 Validation results

To evaluate the redistribution process of residual stress, multi-process milling validation is conducted. Because sub-surface residual stress is difficult to measure directly, only the surface residual stress of the machined part is measured and compared with the analytical results. The analytical results of surface residual stress (FE-σ_{xx} and FE-σ_{yy}) are listed according to the figures, while the distance from the surface is zero. As displayed in Table 4, the calibrated error between the FE model and test measurement is less than 10%, proving the feasibility of the method through FE models. Deformation measurement values in Table 5 provide further evidence of the findings.

5 Conclusion

Process parameters are critical to residual stress and deflection in multi-process milling. In this paper, a multi-process analysis is presented to investigate the redistribution mechanism of residual stress. Simulation models of the machining process and heat treatment are carried out to examine residual stress and deformation, after which an experimental test is conducted to verify the model results. By combining theory analysis and experiments, this study investigates redistribution residual stress during multi-process milling of thin-walled parts. The following conclusions can be drawn:

(1) During milling, various processing parameters will affect the redistribution of residual stress. As the depth of cut declines from semi-finishing to finishing, the machined surface residual stress and deformation reduce accordingly.

(2) To reduce residual stress in multi-process milling, heat treatment is recommended between every cutting process to optimize redistributed residual stress. The residual stress of σ_{xx} and σ_{yy} reduces on the surface and tends to become stable on the sub-surface. Although the sub-surface residual stress σ_{yy} after heat treatment in finishing increases slightly on the sub-surface residual, 10 MPa has less effect on the sub-surface.

Table 4 Surface residual stress validation results

	Semi-finishing process	Semi-finishing process with heat treatment	Finishing process	Finishing process with heat treatment
FE-σ_{xx} (MPa)	17.6	5.5	− 55.8	− 16.7
Test-σ_{xx} (MPa)	16.1	6.0	− 61.2	− 18.1
FE-σ_{yy} (MPa)	− 90.1	− 45.2	− 30.2	− 17.1
Test-σ_{yy} (MPa)	− 84.6	− 49.6	− 27.8	− 16.6

Table 5 Plate deformation validation results

Max deformation of the workpiece plate (mm)	Semi-finishing process	Semi-finishing process with heat treatment	Finishing process	Finishing process with heat treatment
FE-X direction	0.1670	0.0611	0.0633	0.0325
Test-X direction	0.1920	0.0710	0.0720	0.0330
FE-Y direction	0.1072	0.01032	0.0576	0.0270
Test-Y direction	0.1220	0.01120	0.0680	0.0310

(3) After the thin-walled workpiece is processed in multi-processes with heat treatment, surface compressive stress of the thin-walled workpiece is greatly reduced and sub-surface residual stress of the thin-walled workpiece quickly enters into a stable state. Thus, the internal metal structure is more reliable and the final deformation is controlled at a low level. Consequently, the machining accuracy of the thin-walled part is improved by optimizing the redistribution of residual stress.

Funding information This study was financially supported by the Shanghai Sailing Program (no. 18YF1418400).

References

1. Gao H, Zhang Y, Wu Q, Li B (2018) Investigation on influences of initial residual stress on thin-walled part machining deformation based on a semi-analytical model. J. Mater. Process. Technol. 262:437–448
2. Wu C, Pang J, Li B, Liang SY (2019) High speed grinding of HIP-SiC ceramics on transformation of microscopic features. Int. J. Adv. Manuf. Technol. https://doi.org/10.1007/s00170-018-03226-4
3. Arrazola PJ, Özel T, Umbrello D, Davies M, Jawahir IS (2013) Recent advances in modelling of metal machining processes. CIRP Ann.: Manuf. Technol. 62:695–718
4. Coto B, Navas VG, Gonzalo O, Aranzabe A, Sanz C (2011) Influences of turning parameters in surface residual stresses in AISI 4340 steel. Int. J. Adv. Manuf. Technol. 53:911–919
5. Navas VG, Gonzalo O, Bengoetxea I (2012) Effect of cutting parameters in the surface residual stresses generated by turning in AISI4340 steel. Int. J. Mach. Tools Manuf. 61:48–57
6. Li J, Jing L, Chen M (2009) An FEM study on residual stresses induced by high-speed end-milling of hardened steel SKD11. J. Mater. Process. Technol. 209(9):4515–4520
7. Masoudi S, Amini S, Saeidi E, Eslami-Chalander H (2015) Effect of machining-induced residual stress on the deformation of thin-walled parts. Int. J. Adv. Manuf. Technol. 76(1-4):597–608
8. Huang K, Yang W, Ye X (2018) Adjustment of machining-induced residual stress based on parameter inversion. Int. J. Mech. Sci. 135:43–52
9. Jiang X, Zhu Y, Zhang Z, Guo M, Ding Z (2018) Investigation of residual impact stress and its effects on the precision during milling of the thin-walled part. Int. J. Adv. Manuf. Technol. 97(1-4):877–892
10. Zhang J, Lin B, Fei J, Huang T, Xiao J, Zhang X, Ji C (2018) Modeling and experimental validation for surface error caused by axial cutting force in end-milling process. Int. J. Adv. Manuf. Technol. 98(1-4):213–222
11. Kazban RV (2006) Effect of tool parameters on residual stress and temperature generation in high-speed machining of aluminum alloys. Dissertations & Theses – Gradworks 8(2):1120–1120
12. Mohamed NA, Ng E-G, Elbestawi MA (2007) Modelling the effects of tool-edge radius on residual stresses when orthogonal cutting AISI 316L. Int. J. Mach. Tools. Manuf. 47(2):401–411
13. Tang Z, Liu Z, Pan Y, Wan Y, Ai X (2009) The influence of tool flank wear on residual stresses induced by milling aluminum alloy. J. Mater. Process. Technol. 09(2):4502–4508
14. Muñoz-Sánchez A, Canteli JA, Cantero JL, Miguélez MH (2011) Numerical analysis of the tool wear effect in the machining induced residual stresses. Simul. Model Pract. Th. 19:872–886
15. Huang K, Yang W (2017) Analytical analysis of the mechanism of effects of machining parameter and tool parameter on residual stress based on multivariable decoupling method. Int. J. Mech. Sci. 128:659–679
16. Jiang X, Zhang Z, Ding ZO (2017) F., Liang, S.Y., Tool overlap effect on redistributed residual stress and shape distortion produced by the machining of thin-walled aluminum parts. Int. J. Adv. Manuf. Technol. 93(5-8):2227–2242
17. Treuting RG, Read WT (1951) A mechanical determination of biaxial residual stress in sheet materials. J. Appl. Phys. 22(2):130–134
18. Liu C, Guo Y (2000) Finite element analysis of the effect of sequential cuts and tool-chip friction on residual stresses in a machined layer. Int. J. Mech. Sci. 42:1069–1086
19. Lee HY, Nikbin KM (2007) Modelling the redistribution of residual stresses at elevated temperature in components. Fatigue Fract. Mech. 35:54–68
20. Robinson JS, Tanner DA, Truman CE, Wimpory RC (2011) Measurement and prediction of machining induced redistribution of residual stress in the aluminium alloy 7449. Exp. Mech. 51:981–993
21. Li B, Jiang X, Yang J, Liang SY (2015) Effects of depth of cut on the redistribution of residual stress and deformation during the milling of thin-walled part. J. Mater. Process. Technol. 216:223–233
22. Third Wave Systems, 2010 Inc., AdvantEdge V5.6-014 machining simulation software. Minneapolis, MN. .
23. Abaqus I, Systemes D (2013) Analysis user's manual, version 6.13. Simulia, Paris
24. Ulutan D, Alaca BE, Lazoglu I (2007) Analytical modeling of residual stresses in machining. J Mater Process Technol. 183:77–87
25. Lazoglu I, Ulutan D, Alaca BE, Engin S, Kaftanoglu B (2008) An enhanced analytical model for residual stress prediction in machining. CIRP Annals - Manuf Technol. 57:81–84
26. Liang SY, Su JC (2007) Residual stress modeling in orthogonal machining. CIRP Annals - Manuf Technol 56(1):65–68